Electronic Supplementary Information for Dalton Transactions

Supporting Information

Mechanistic information from volume profiles for water exchange and complex-formation reactions of aquated Ni(II). pH, buffer and medium effects

Hanaa Asaad Gazzaz, Erika Ember, Achim Zahl and Rudi van Eldik*

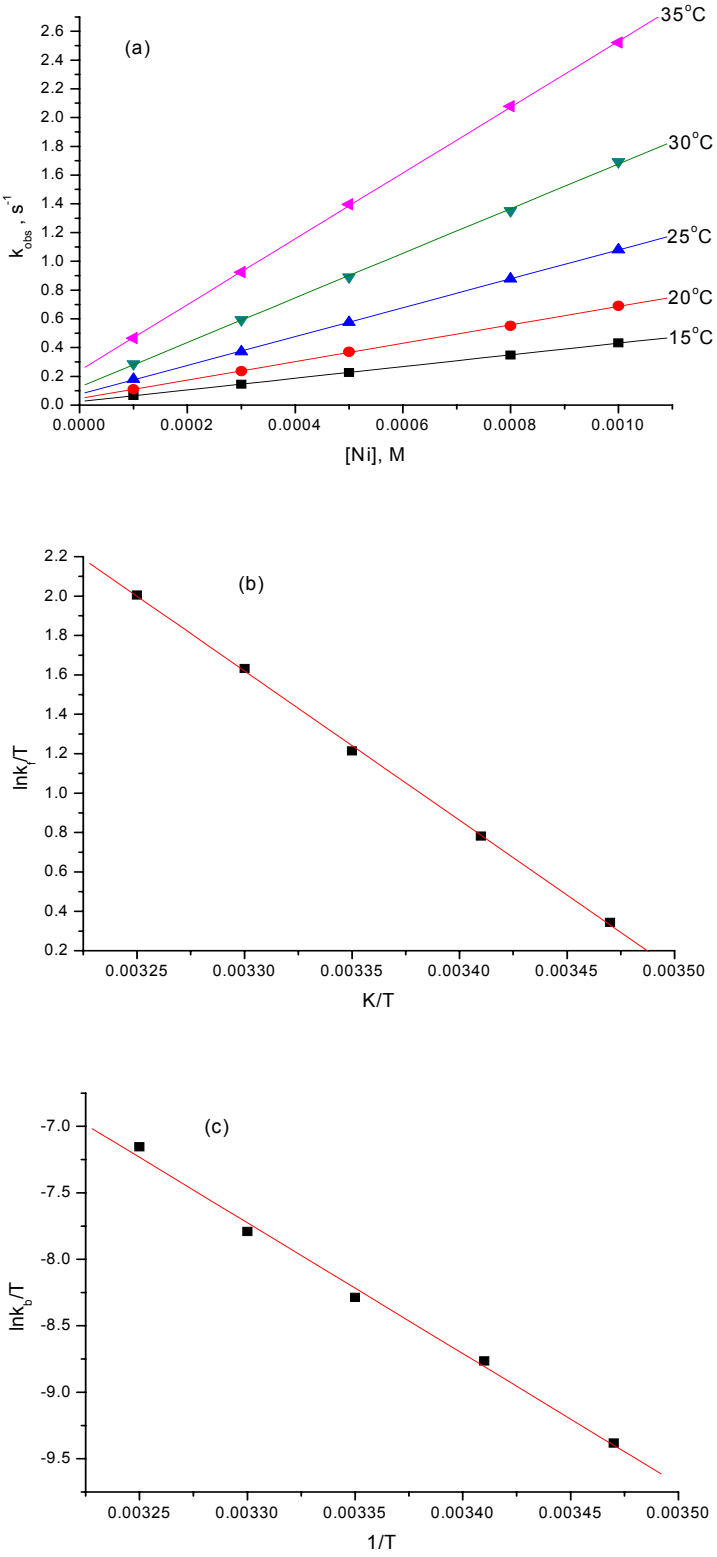

Figure S1. (a) Variation of the observed rate constant k_{obs} with Ni^{2+} concentration for the reaction between Ni^{2+} and 1×10^{-5} M PADA in 0.05 M MES buffer at pH 6, under ambient pressure and at different temperatures. (b) and (c) Eyring plots for the

forward rate constant k_f and the backward rate constant k_b of the reaction in (a), respectively.

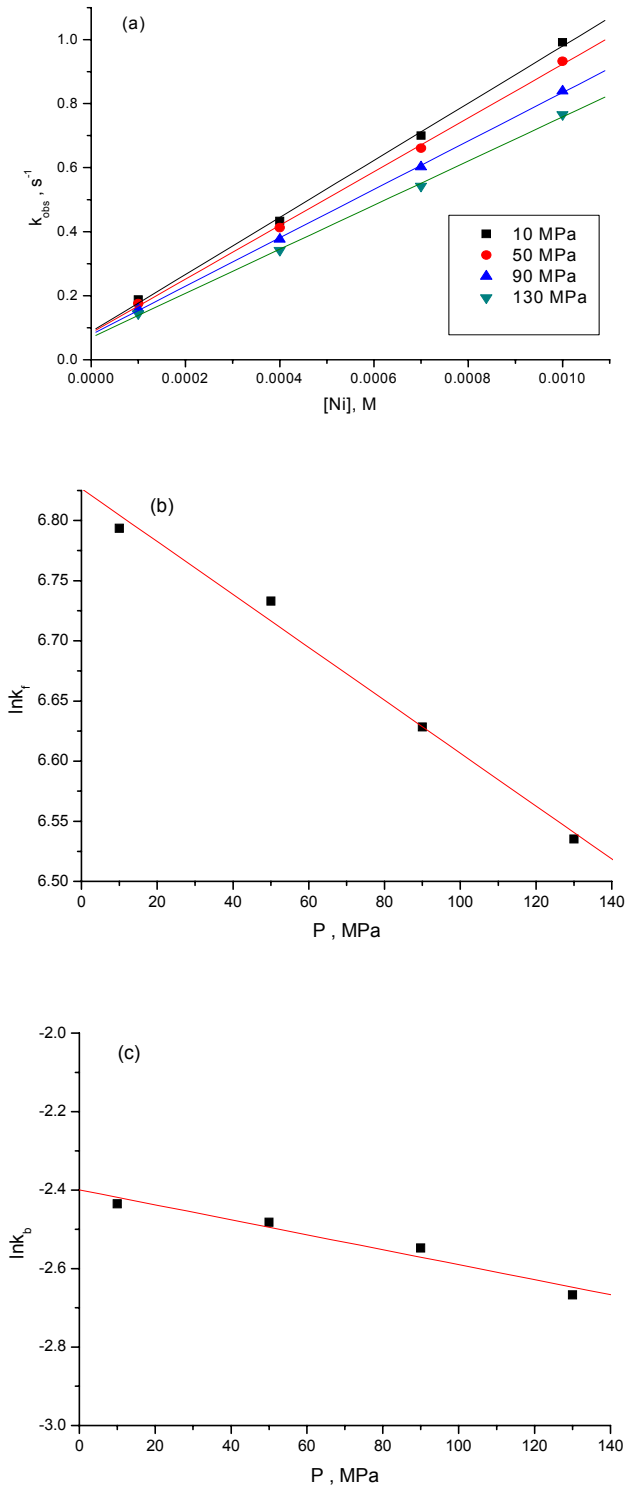

Figure S2. (a) Variation of the observed rate constant k_{obs} with Ni^{2+} concentration for the reaction between Ni^{2+} and 1×10^{-5} M PADA in 0.05 M MES buffer at pH 6, 25 ^{o}C and different pressures. (b) and (c) Pressure dependence of the forward rate constant k_f and the backward rate constant k_b for the reaction in (a), respectively.

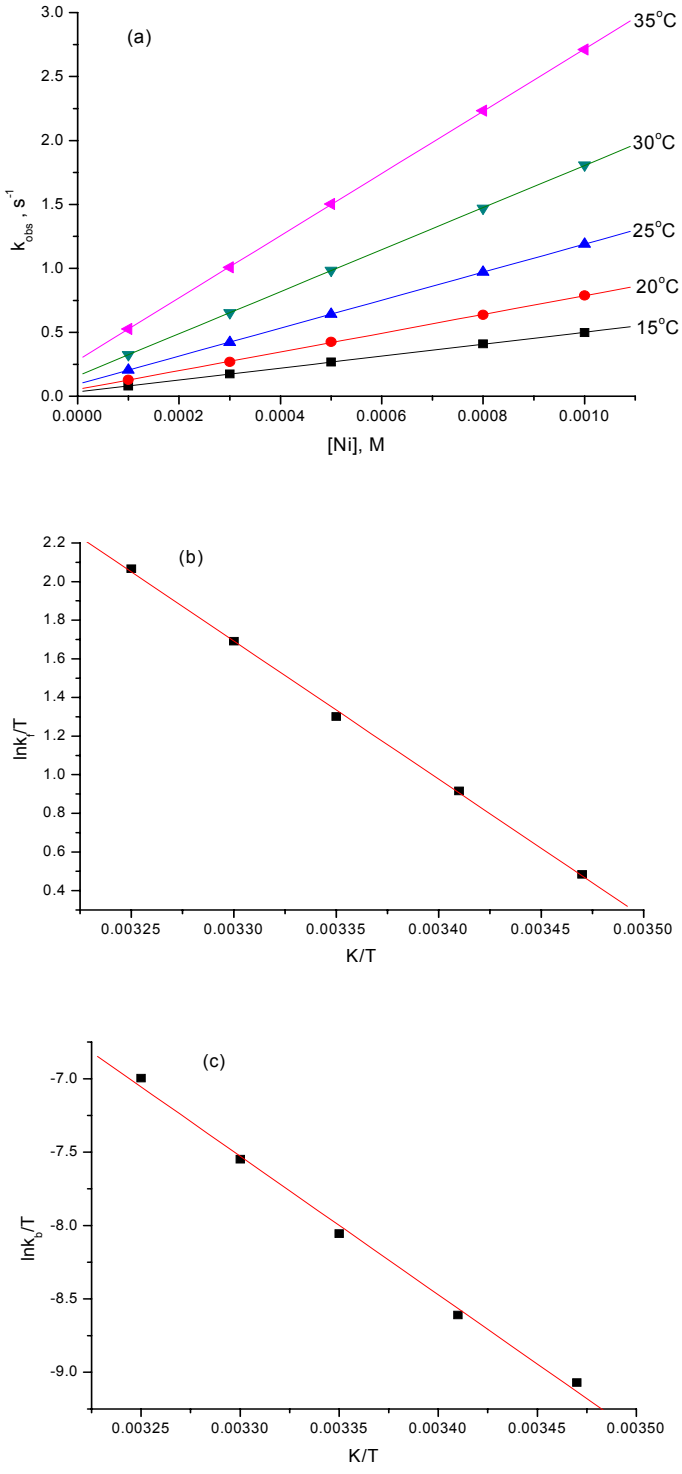

Figure S3. (a) Variation of the observed rate constant k_{obs} with Ni^{2+} concentration for the reaction between Ni^{2+} and 1×10^{-5} M PADA in 0.05 M Tris buffer at pH 7, at ambient pressure and different temperatures. (b) and (c) Eyring plots for the forward rate constant k_f and the backward rate constant k_b of the reaction in (a), respectively.

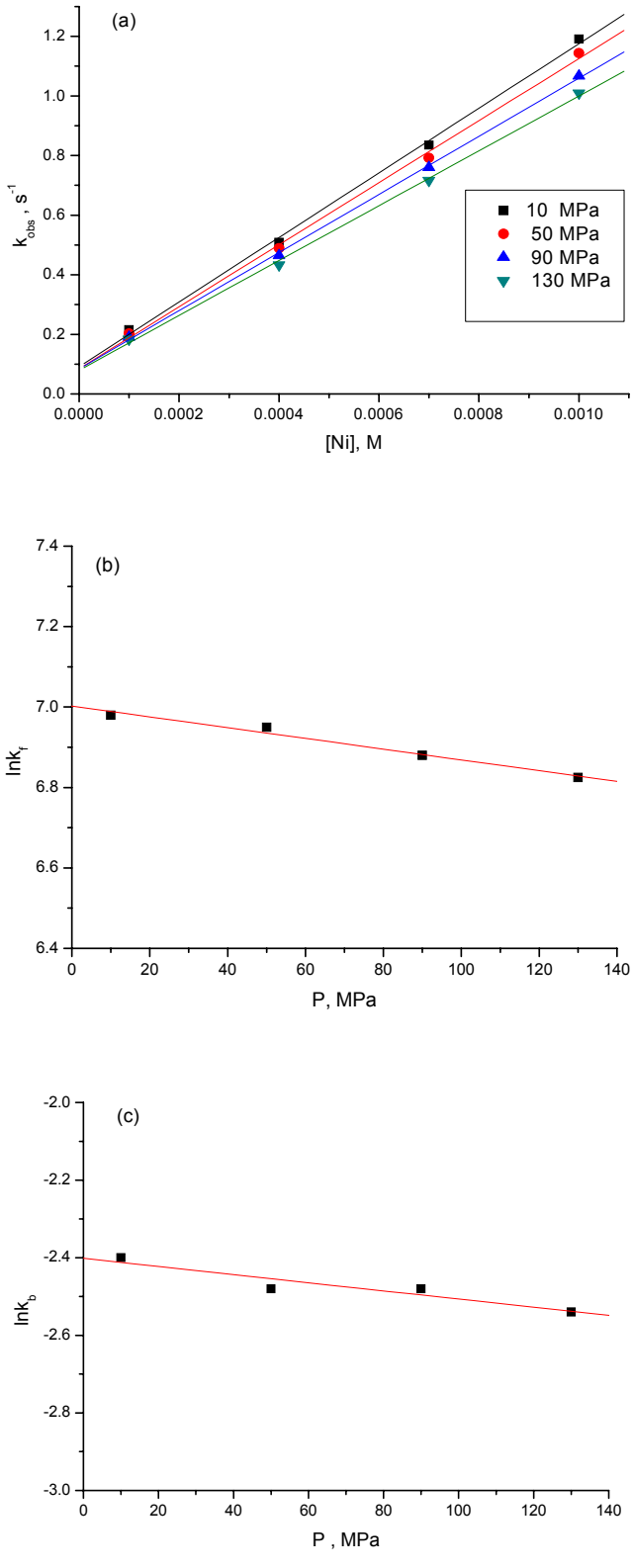

Figure S4. (a) Variation of the observed rate constant k_{obs} with Ni^{2+} concentration for the reaction between Ni^{2+} and 1×10^{-5} M PADA in 0.05 M Tris buffer at pH 7, 25 ^{o}C

and different pressures. (b) and (c) Pressure dependence of the forward rate constant k_f and the backward rate constant k_b for the reaction in (a), respectively.

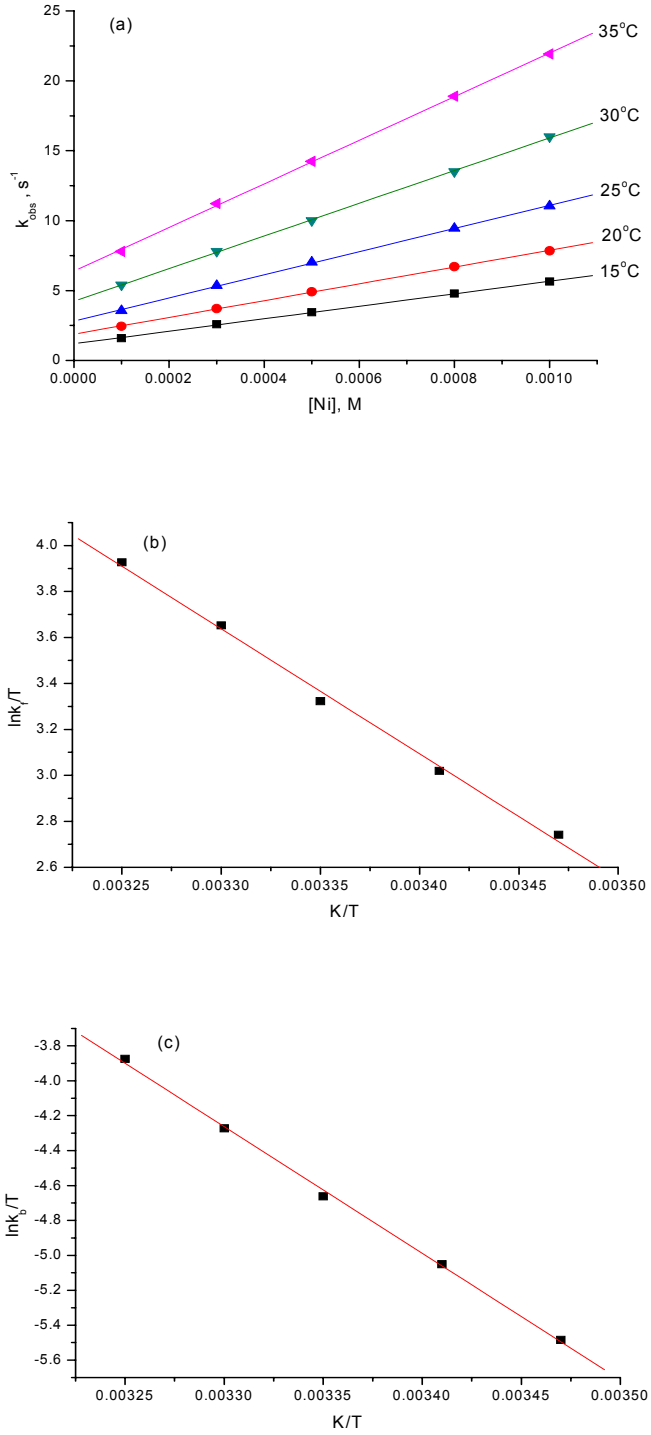

Figure S5. (a) Variation of the observed rate constant k_{obs} with Ni^{2+} concentration for the reaction between Ni^{2+} and 1×10^{-5} M PADA in 0.05 M Tris buffer at pH 9, ambient pressure and different temperatures. (b) and (c) Eyring plots for the forward rate constant k_f and the backward rate constant k_b of the reaction in (a), respectively.

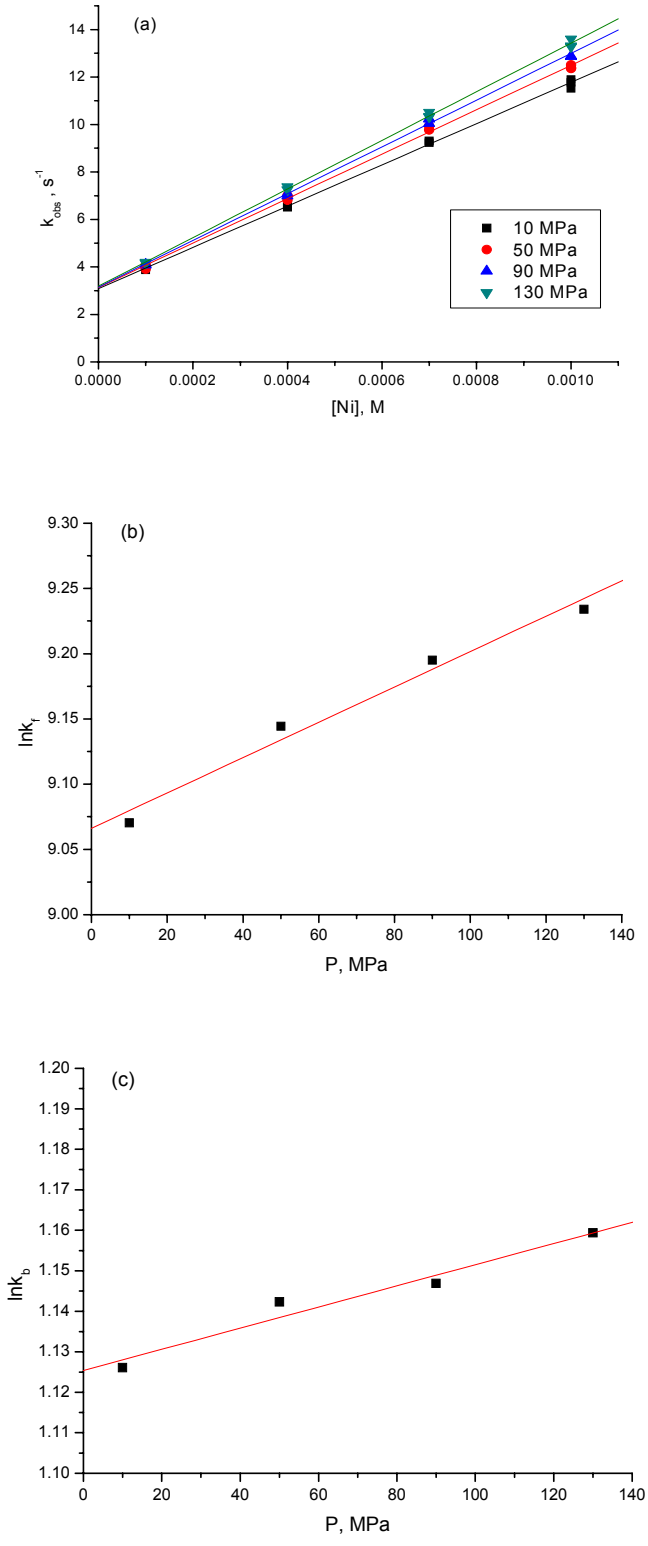

Figure S6. (a) Variation of the observed rate constant k_{obs} with Ni^{2+} concentration for the reaction between Ni^{2+} and 1×10^{-5} M PADA in 0.05 M Tris buffer at pH 9, 25 ^{o}C and different pressures. (b) and (c) Pressure dependence of the forward rate constant k_f and the backward rate constant k_b for the reaction in (a), respectively.

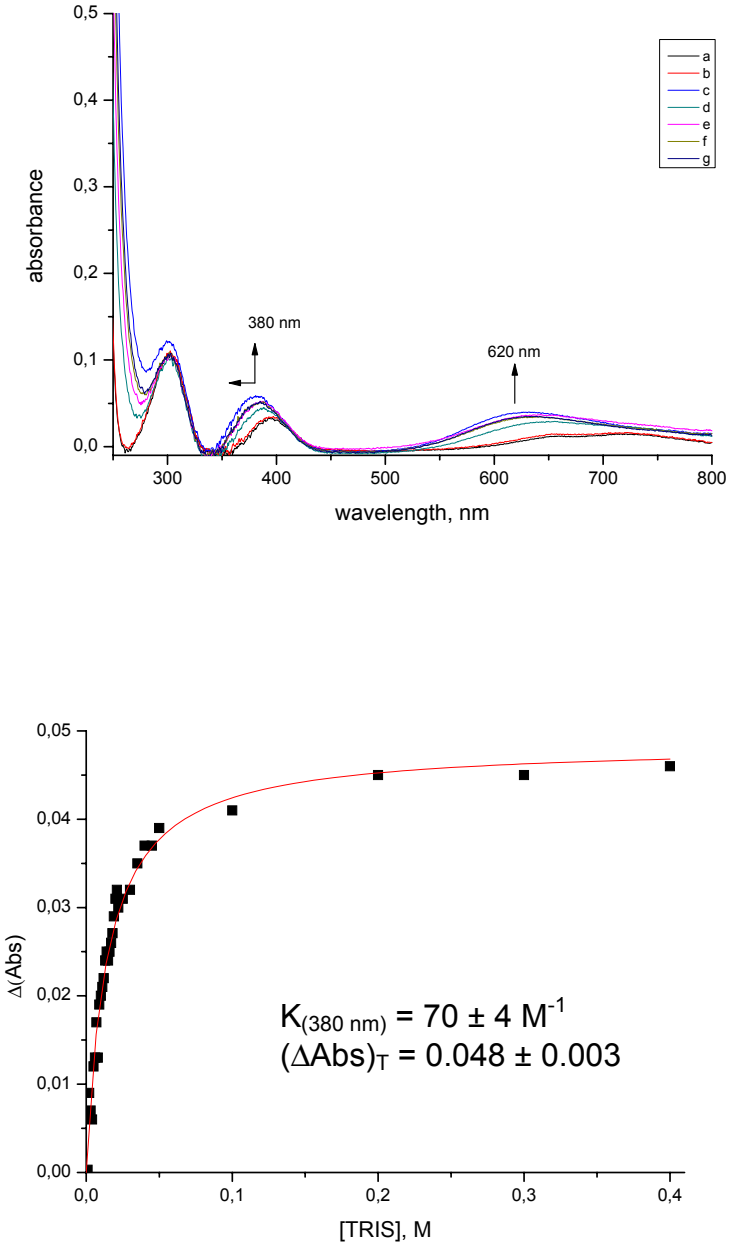

Figure S7. Spectrophotometric titration (top) and plot of the absorbance change at 380 nm that accompanies the complex-formation reaction as a function of Tris concentration (bottom). Experimental conditions: 10 mM Ni^{2+}, (a) reference spectra, (b) 1 mM Tris, (c) 100 mM Tris, (d) 200 mM Tris, (e) 300 mM Tris, (f) 400 mM Tris, (g) 500 mM Tris, pH = 9 and 25 °C.

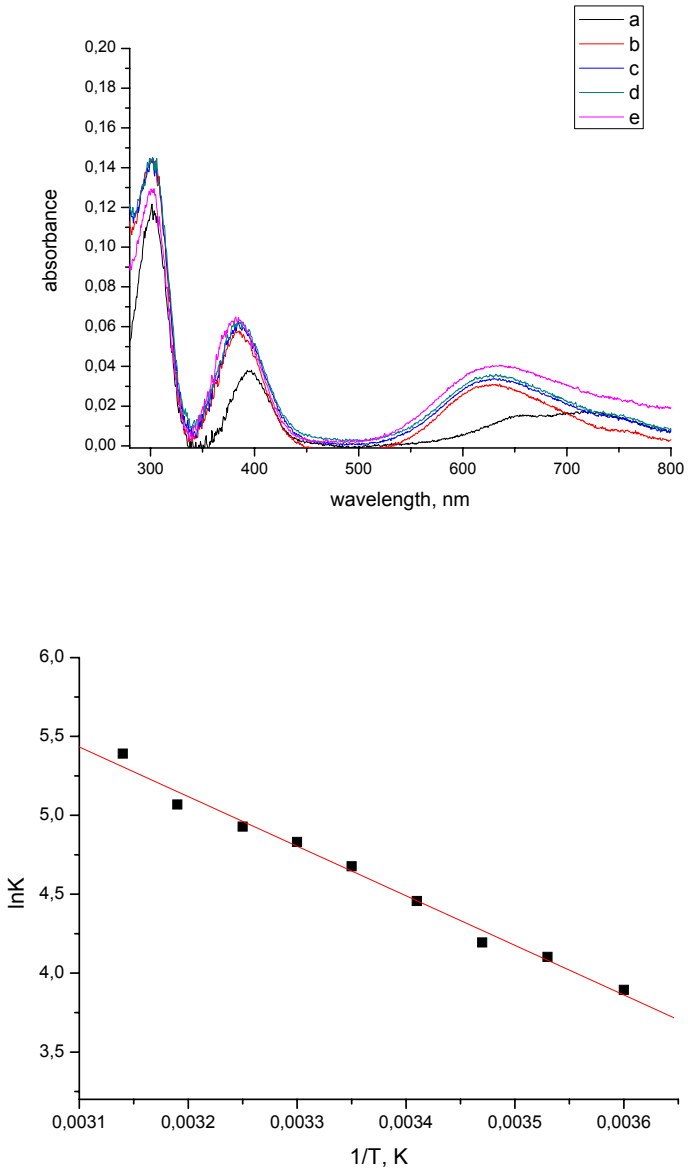

Figure S8. Effect of temperature on the complex-formation of Ni^{2+} by Tris at pH = 9 (top) and plot of lnK versus 1/T (bottom). Experimental conditions: 10 mM Ni^{2+}, 25 mM Tris, spectrum of reactants before mixing (a) and after mixing (b) at 10 °C, (c) 20 °C, (d) 30 °C and (e) 40 °C, respectively, and λ = 380 nm. The resulting thermodynamic parameters are $\Delta H° = 26 \pm 2$ kJ mol^{-1} and $\Delta S° = +126 \pm 3$ J K^{-1} mol^{-1}.

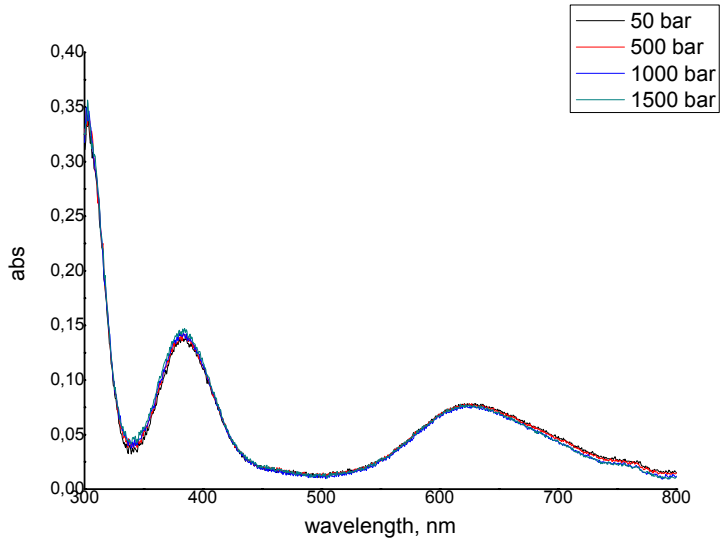

Figure S9. Effect of pressure on the Ni^{2+}-Tris complex-formation equilibrium at pH = 9. Experimental conditions: 10 mM Ni^{2+}, 25 mM Tris and 25 °C.

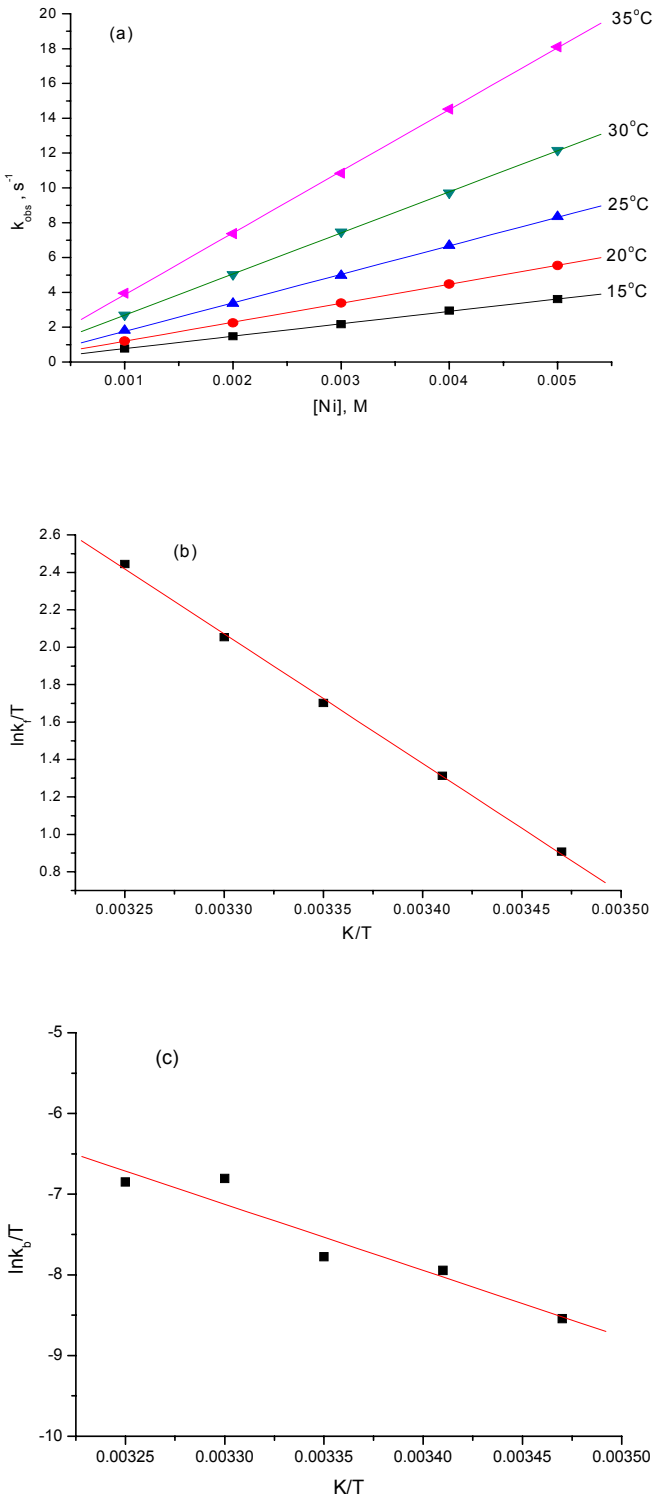

Figure S10. (a) Variation of the observed rate constant k_{obs} with Ni^{2+} concentration for the reaction between Ni^{2+} and 5×10^{-5} M Bipy in 0.05 M Tris buffer at pH 7,

ambient pressure and different temperatures. (b) and (c) Eyring plots for the forward rate constant k_f and the backward rate constant k_b of the reaction in (a), respectively.

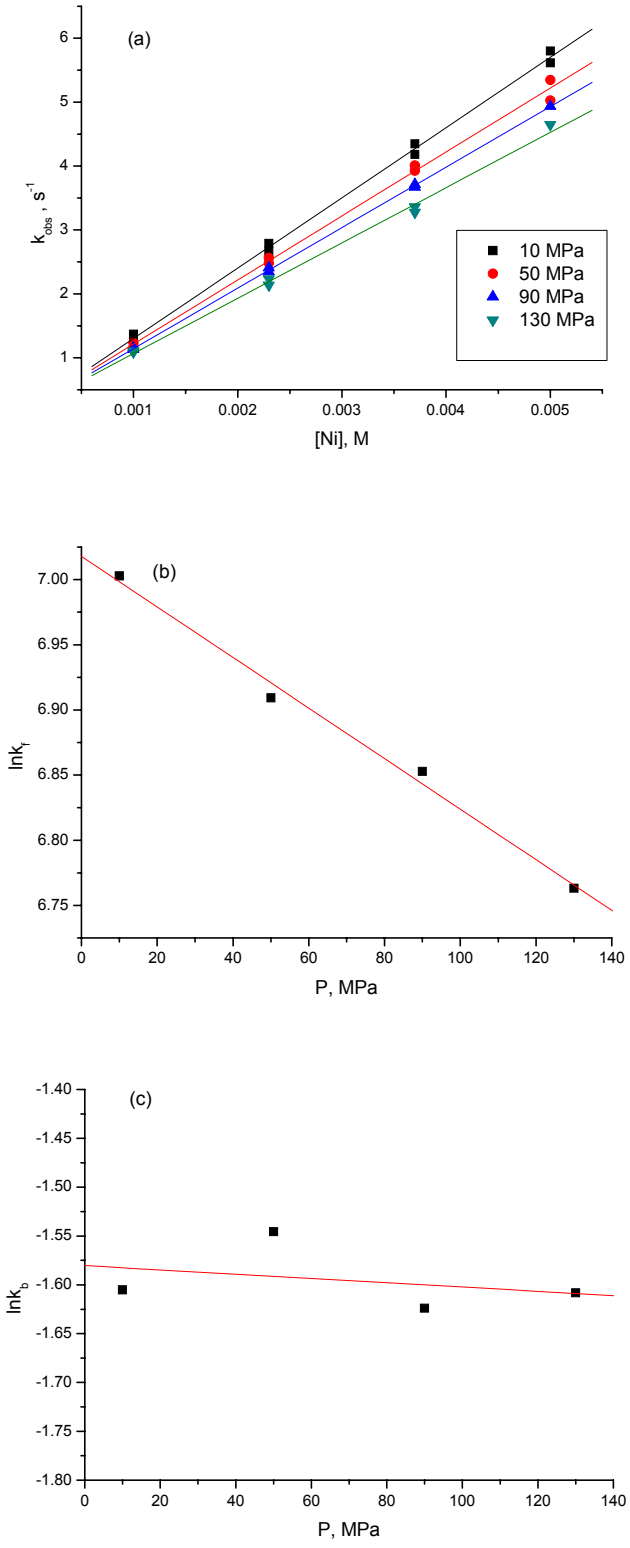

Figure S11. (a) Variation of the observed rate constant k_{obs} with Ni^{2+} concentration for the reaction between Ni^{2+} and 5×10^{-5} M Bipy in 0.05 M Tris buffer at pH 7, 25

^{o}C and different pressures. (b) and (c) Pressure dependence of the forward rate constant k_f and the backward rate constant k_b for the reaction in (a), respectively.

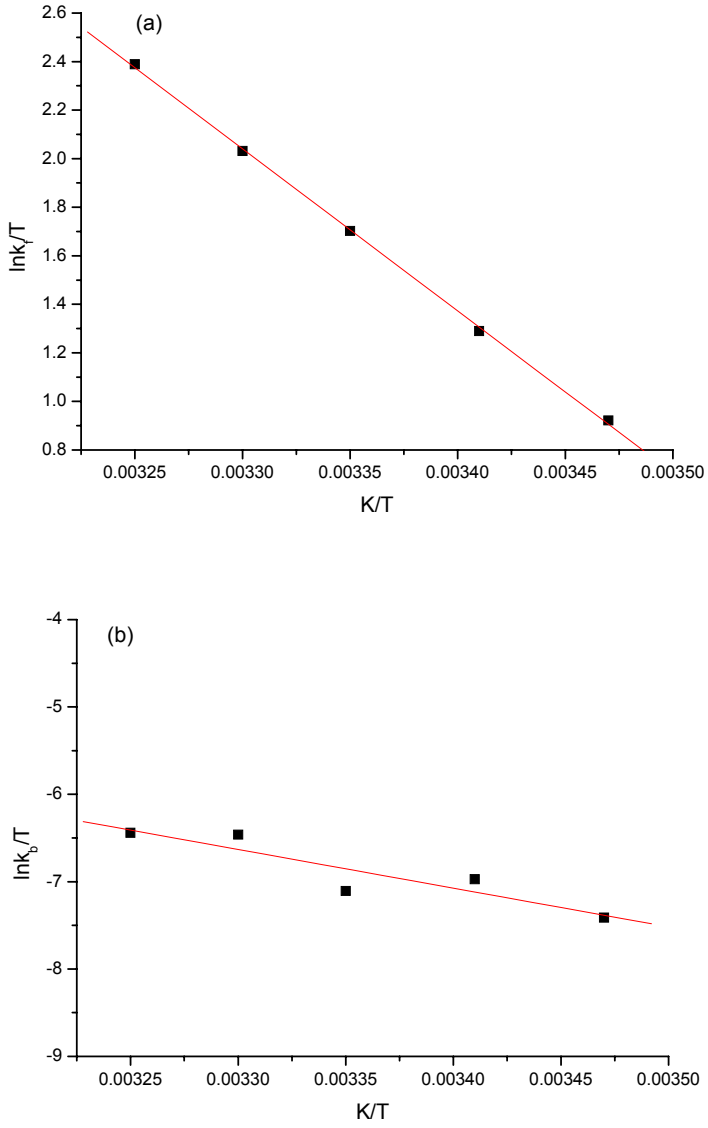

Figure S12. (a) and (b) Eyring plots for the forward rate constant k_f and the backward rate constant k_b of the reaction between Ni^{2+} and 5×10^{-5} M Bipy, respectively, in 0.05 M Tris buffer, pH 8 and at ambient pressure.

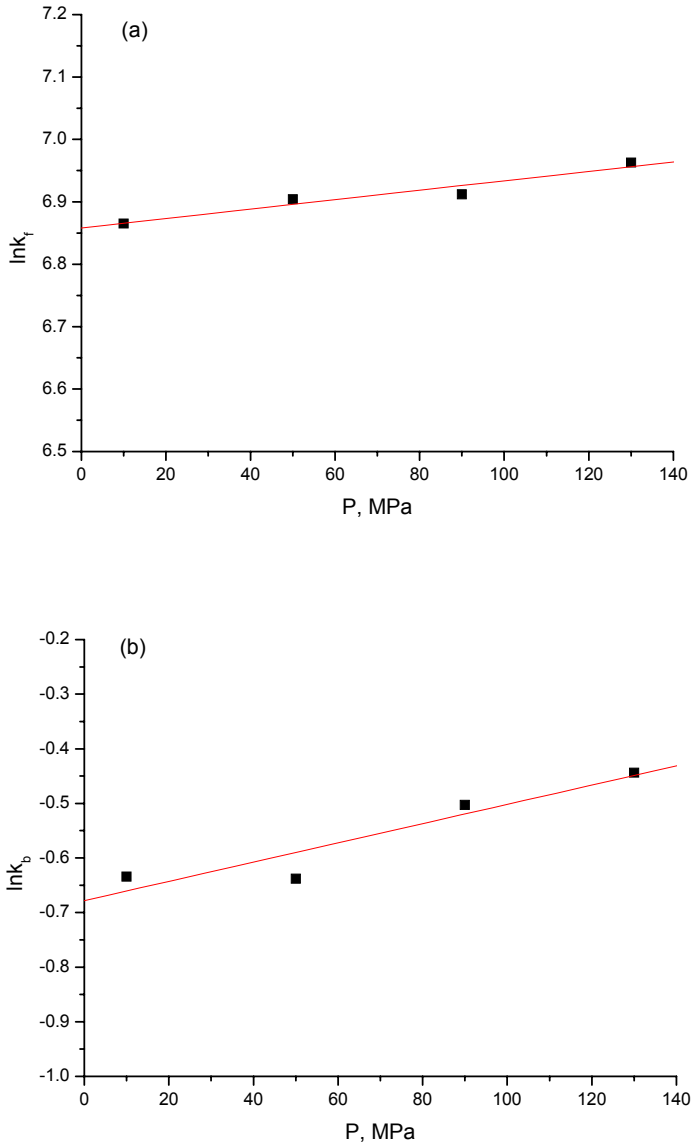

Figure S13. (a) and (b) Pressure dependence of the forward rate constant k_f and the backward rate constant k_b for the reaction between Ni^{2+} and 5×10^{-5} M Bipy, respectively, in 0.05 M Tris buffer at pH 8 and 25 ^{o}C.

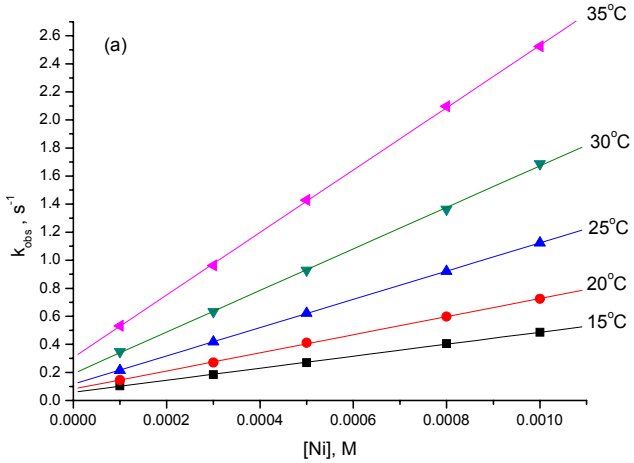

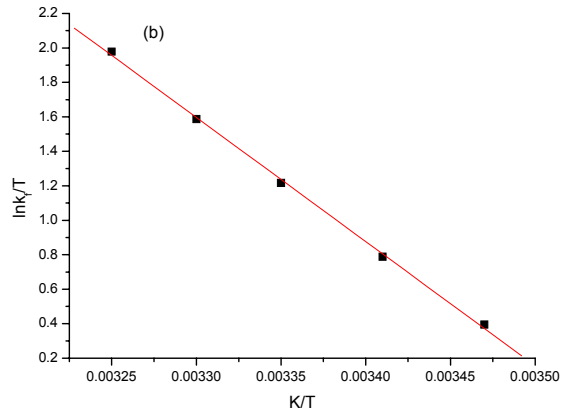

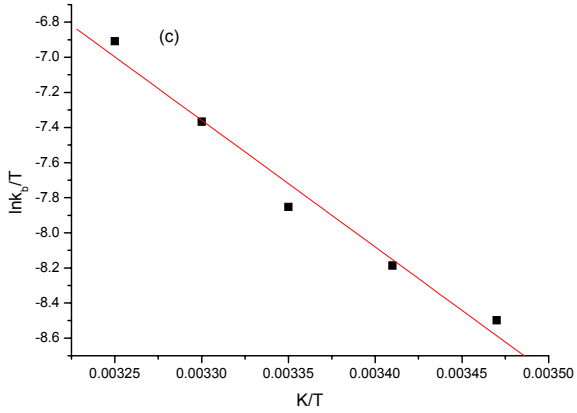

Figure S14. (a) Variation of the observed rate constant k_{obs} with Ni^{2+} concentration for the reaction between Ni^{2+} and 1×10^{-5} M PADA in 0.05 M N-ethylmorpholine buffer at pH 7, ambient pressure and different temperatures. (b) and (c) Eyring plots for the forward rate constant k_f and the backward rate constant k_b of the reaction in (a), respectively.

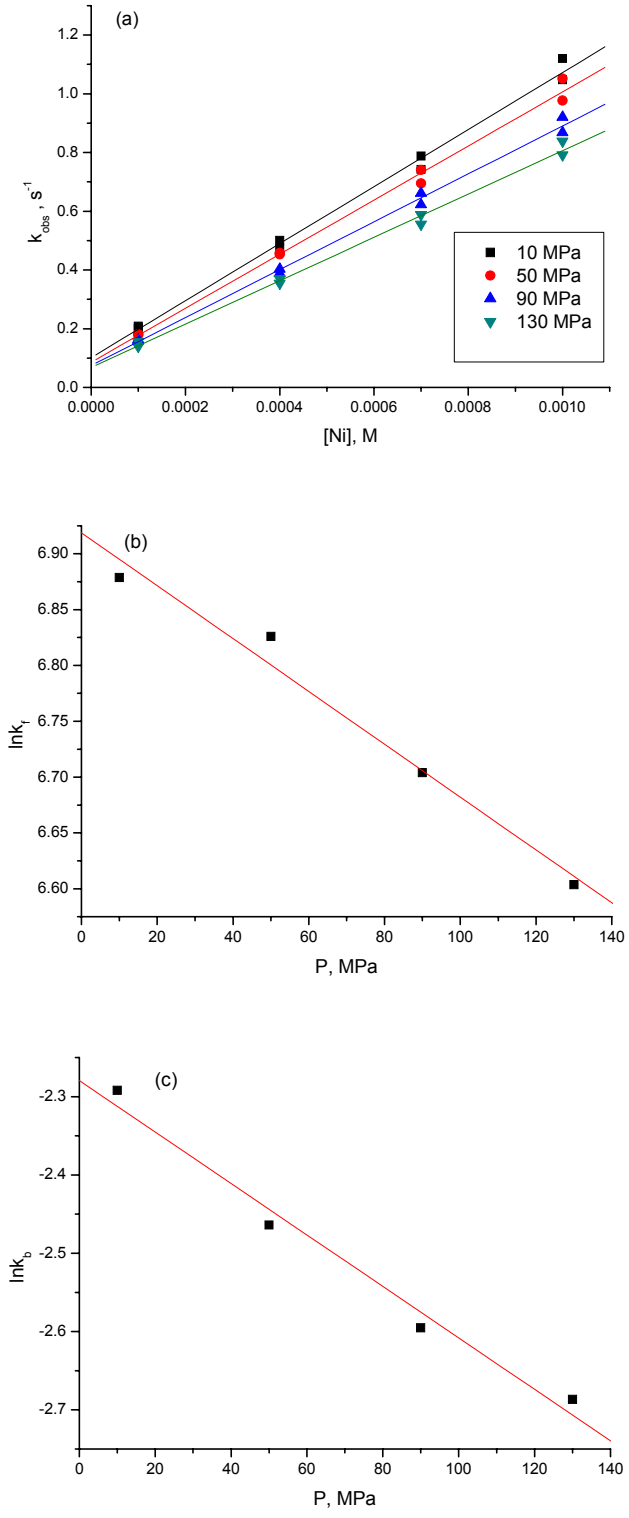

Figure S15. (a) Variation of the observed rate constant k_{obs} with Ni^{2+} concentration for the reaction between Ni^{2+} and 1×10^{-5} M PADA in 0.05 M N-ethylmorpholine buffer at pH 7, 25 ^{o}C and different pressures. (b) and (c) Pressure dependence of the

forward rate constant k_f and the backward rate constant k_b for the reaction in (a), respectively.

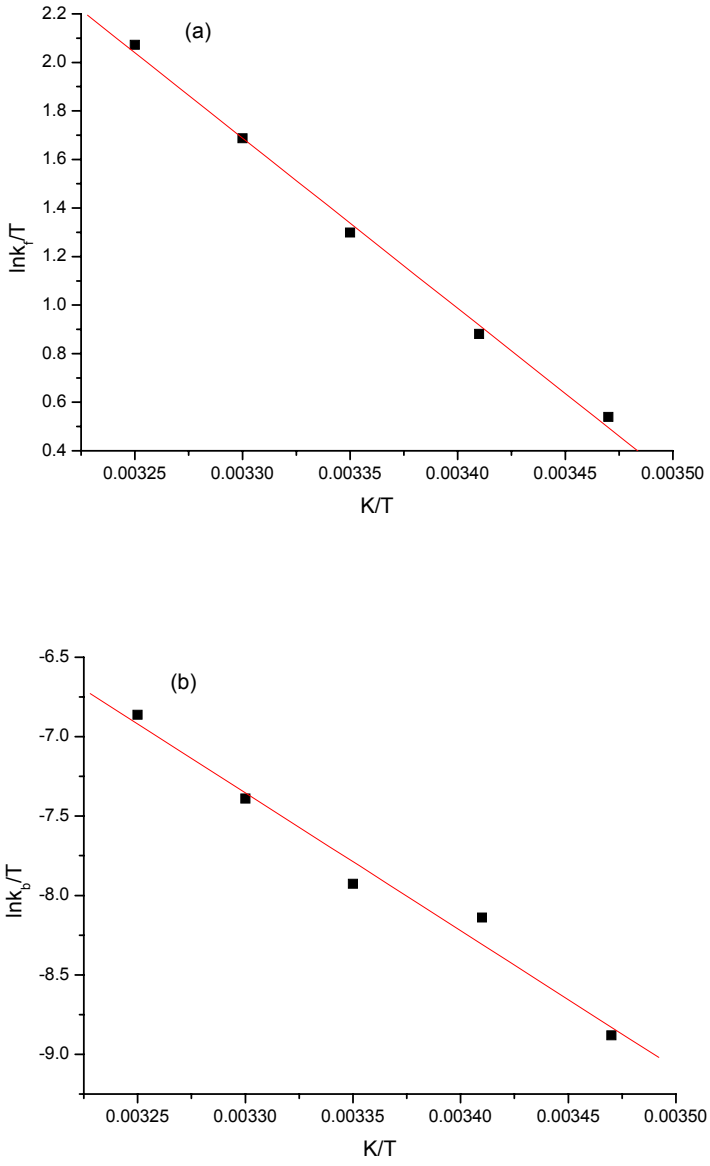

Figure S16. (a) and (b) Eyring plots for the forward rate constant k_f and the backward rate constant k_b of the reaction between Ni^{2+} and 1×10^{-5} M PADA, respectively, in 0.05 M N-ethylmorpholine buffer, pH 8 and at ambient pressure.

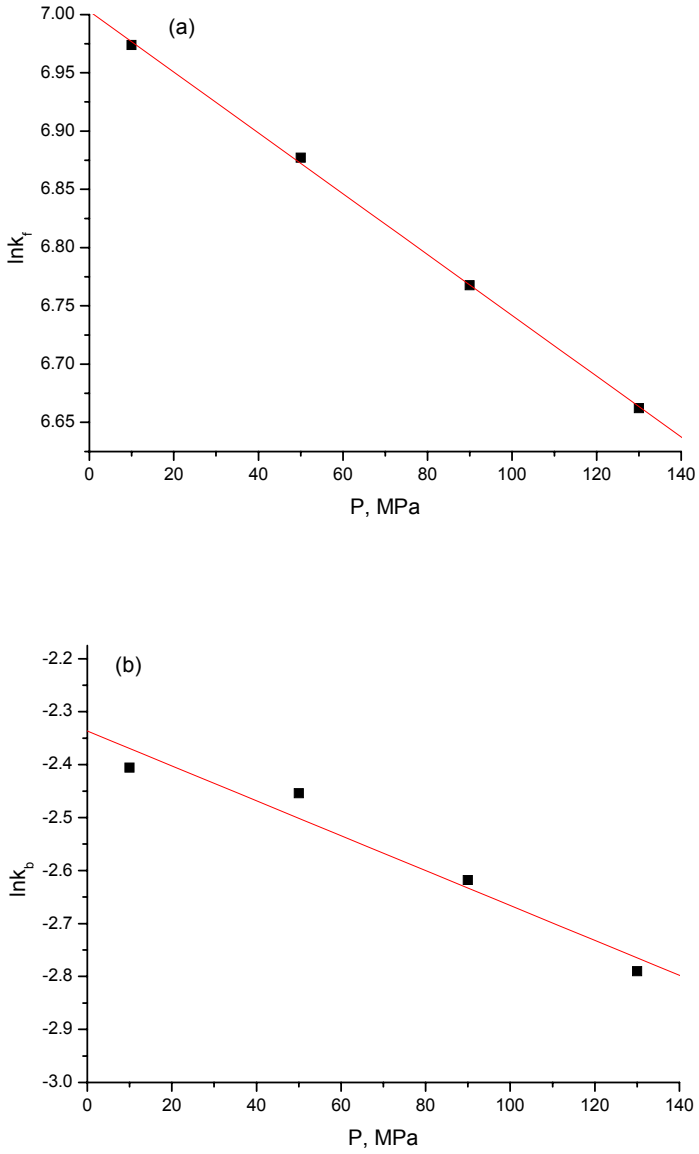

Figure S17. (a) and (b) Pressure dependence of the forward rate constant k_f and the backward rate constant k_b for the reaction between Ni^{2+} and 1×10^{-5} M PADA, respectively, in 0.05 M N-ethylmorpholine buffer, pH 8 and 25 ^{o}C.

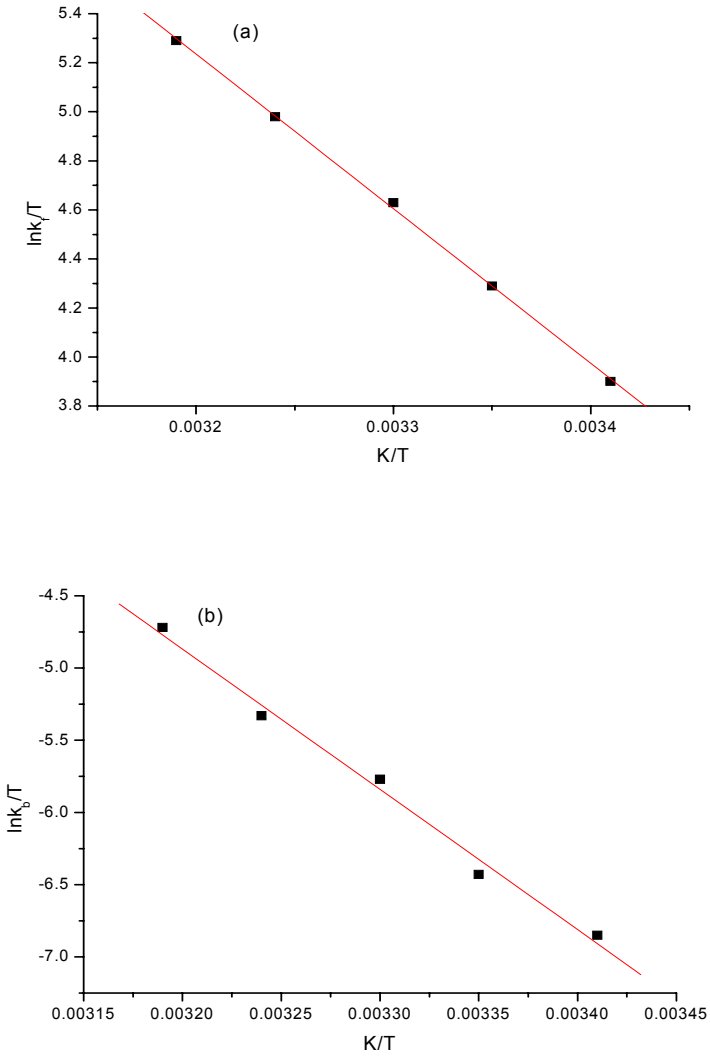

Figure S18. (a) and (b) Eyring plots for the forward rate constant k_f and the backward rate constant k_b of the reaction between Ni^{2+} and 1×10^{-5} M PADA, respectively, in SDS micellar solution, 0.05 M Tris buffer, pH 8 and at ambient pressure.

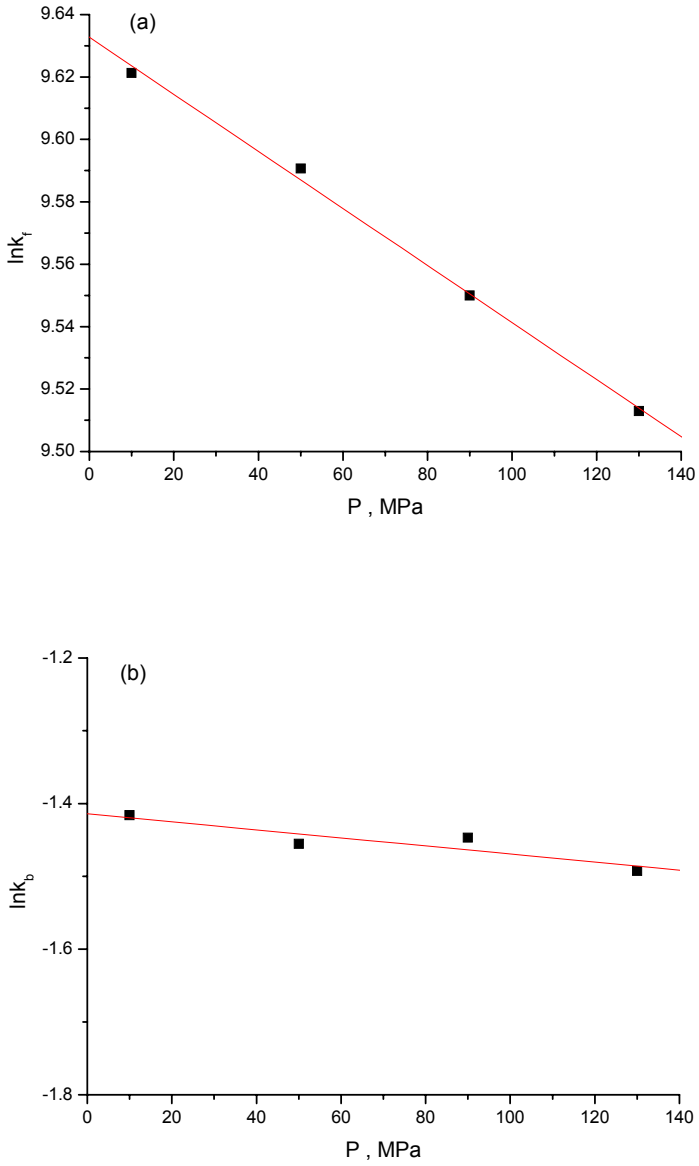

Figure S19. (a) and (b) Pressure dependence of the forward rate constant k_f and the backward rate constant k_b for the reaction between Ni^{2+} and 1×10^{-5} M PADA, respectively, in SDS micellar solution, 0.05 M Tris buffer, pH 8 and 20 ^{o}C.

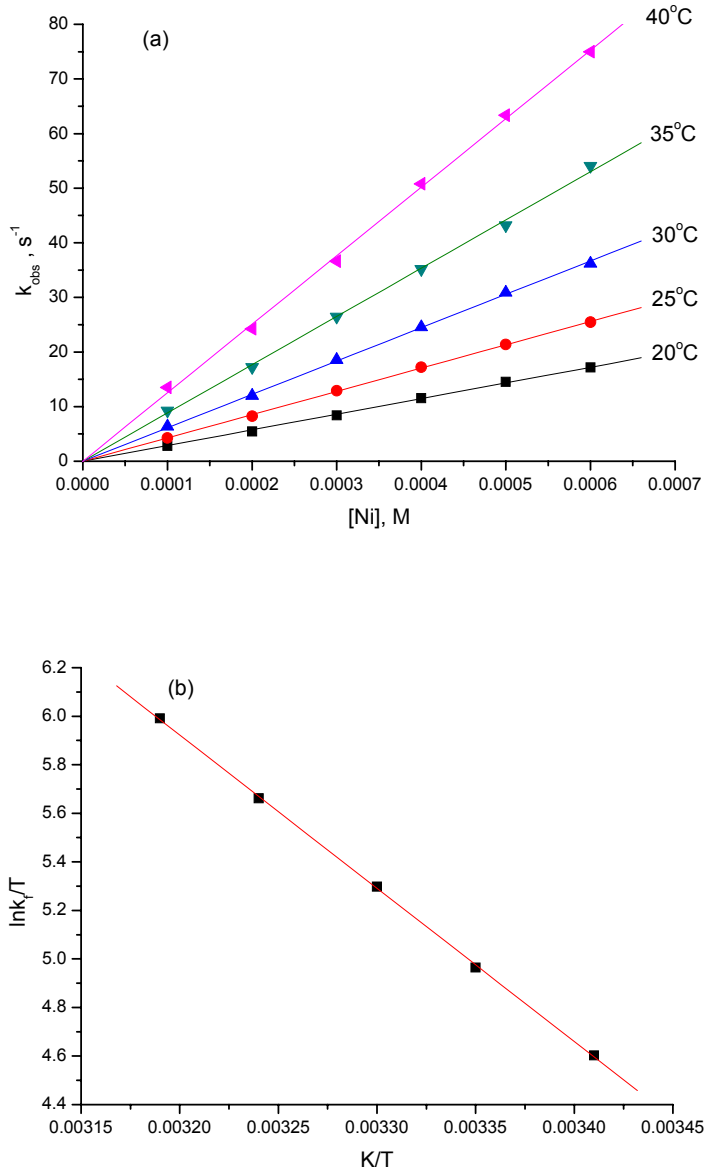

Figure S20. (a) Variation of the observed rate constant k_{obs} with Ni^{2+} concentration for the reaction between Ni^{2+} and PADA in SDS micellar solution at ambient pressure, 0.05 M Tris buffer, pH 9 and different temperatures. (b) Eyring plot for the forward rate constant k_f of the reaction in (a).

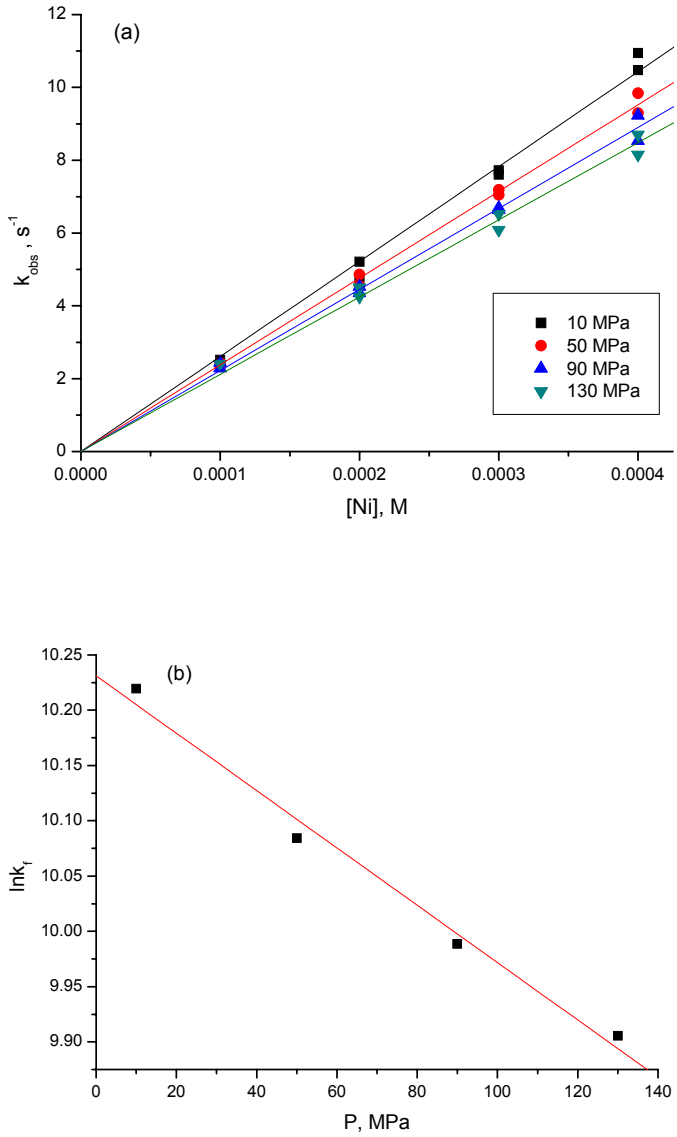

Figure S21. (a) Variation of the observed rate constant k_{obs} with Ni^{2+} concentration for the reaction between Ni^{2+} and PADA in SDS micellar solution at 20 ^{o}C, 0.05 M Tris buffer, pH 9 and different pressures. (b) Pressure dependence of the forward rate constant k_f for the reaction in (a).

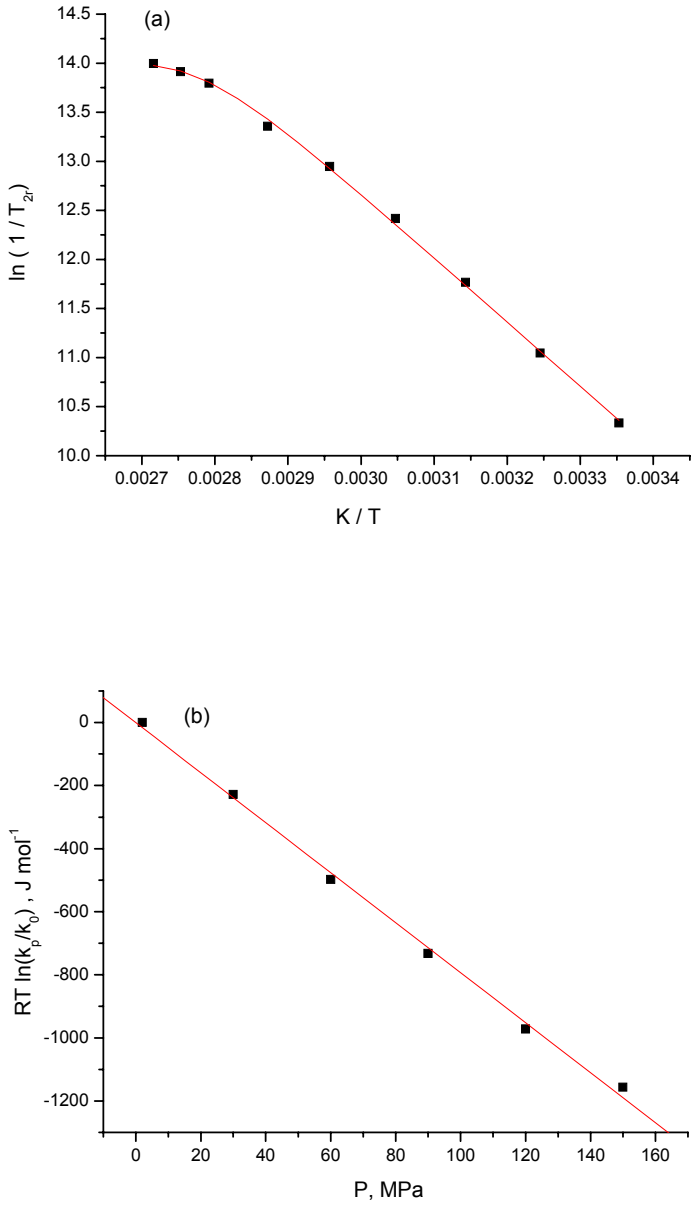

Figure S22. (a) Temperature dependence of the reduced transverse relaxation rate ($1/T_{2r}$) and (b) pressure dependence of the water exchange rate constant k_{ex} for 0.02 M $[Ni(H_2O)_6]^{2+}$ in MES buffer at pH 6 and 45 ^{o}C.

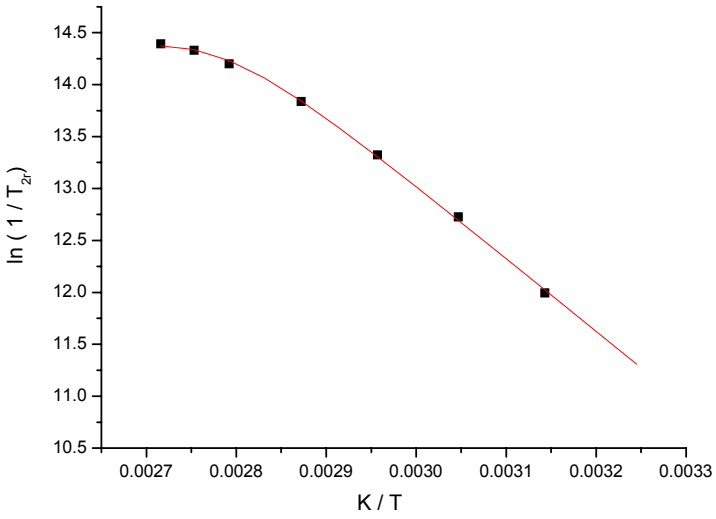

Figure S23. Temperature dependence of the reduced transverse relaxation rate ($1/T_{2r}$) for 0.02 M $[Ni(H_2O)_6]^{2+}$ in Tris buffer at pH 7.

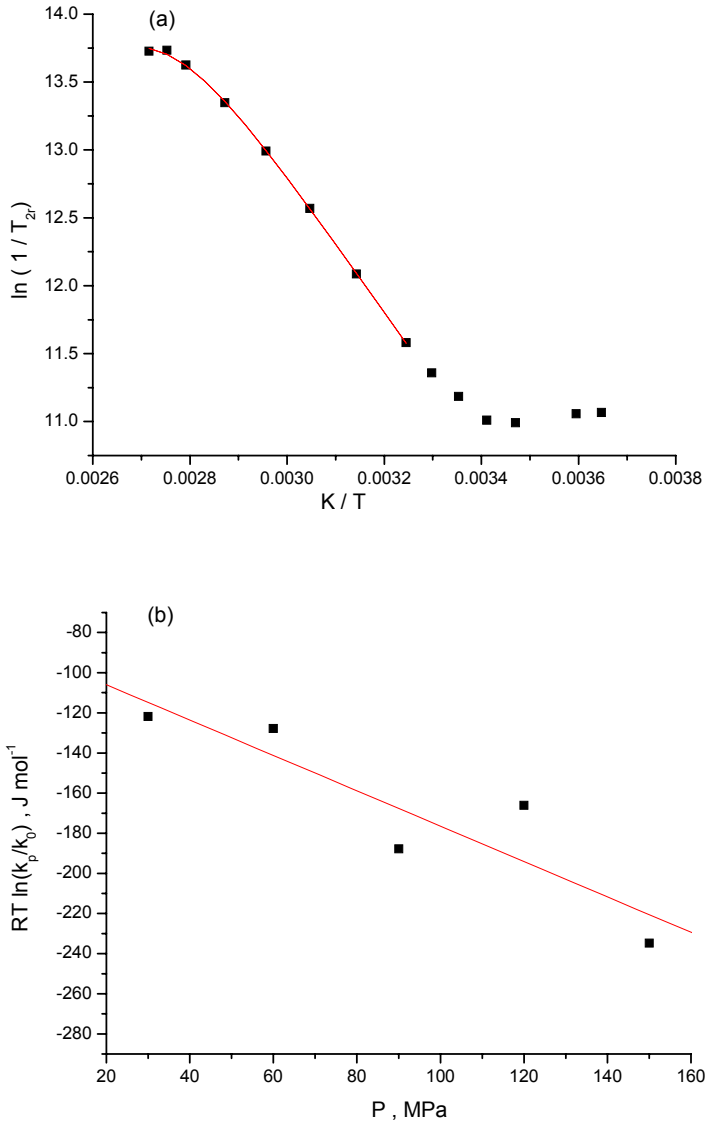

Figure S24. (a) Temperature dependence of the reduced transverse relaxation rate ($1/T_{2r}$) and (b) pressure dependence of the water exchange rate constant k_{ex} for 0.02 M $[Ni(H_2O)_6]^{2+}$ in Tris buffer at pH 9 and 55 ^{o}C. The large scatter in the high pressure data results from the selected scale since the observed pressure effect is indeed very small under these conditions.

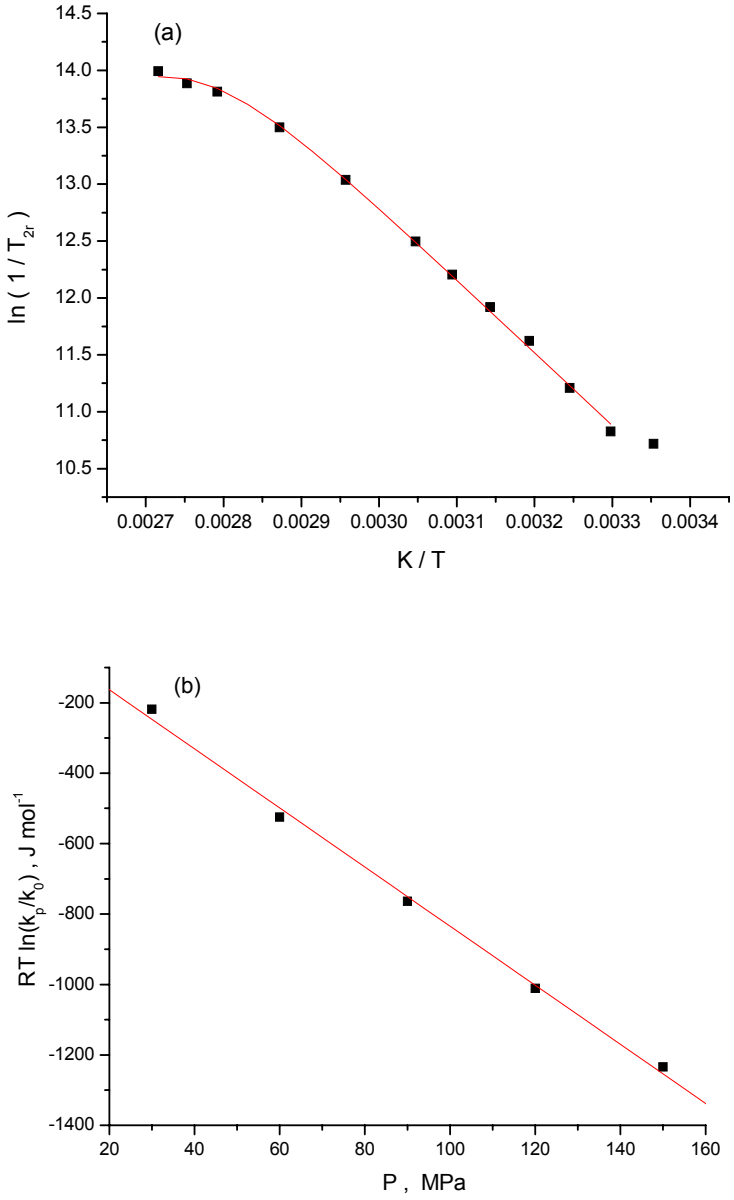

Figure S25. (a) Temperature dependence of the reduced transverse relaxation rate ($1/T_{2r}$) and (b) pressure dependence of the water exchange rate constant k_{ex} for 0.02 M $[Ni(H_2O)_6]^{2+}$ in N-ethylmorpholine buffer at pH 8 and 55 ^{o}C.

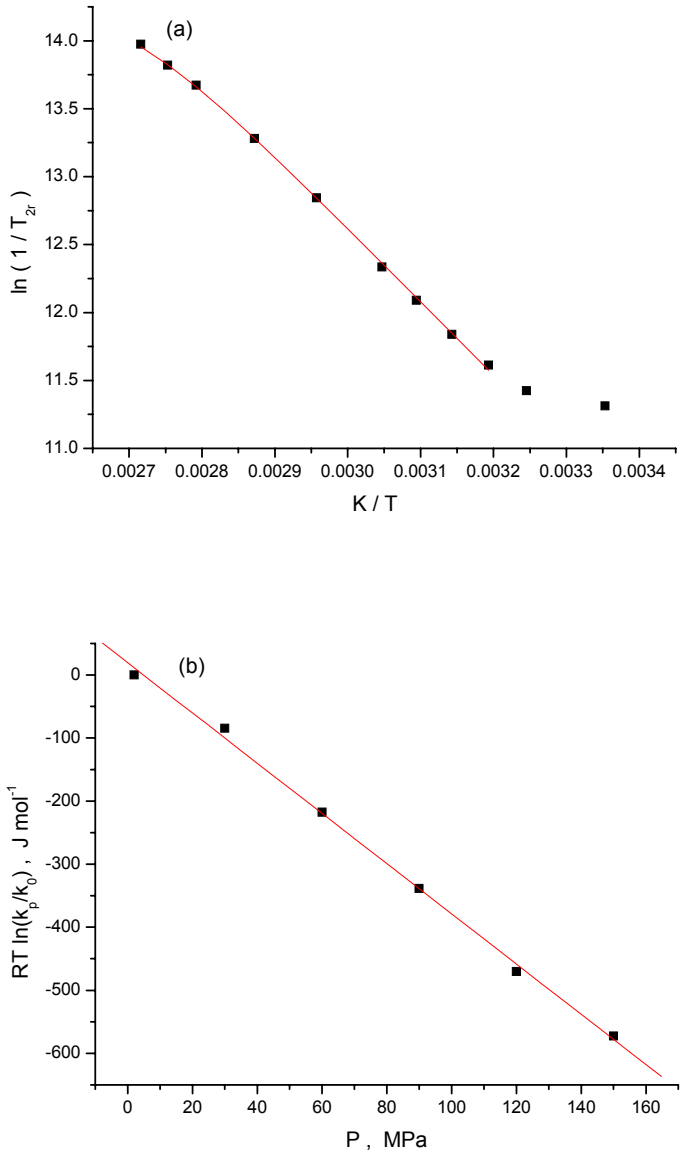

Figure S26. (a) Temperature dependence of the reduced transverse relaxation rate ($1/T_{2r}$) and (b) pressure dependence of the water exchange rate constant k_{ex} of 0.02 M $[Ni(H_2O)_6]^{2+}$ in SDS micellar solution, Tris buffer, pH 8 and 50 ^{o}C.